Optical fingerprints of Y2 ordering in III–V ternary semiconductor alloys

2013 Semicond. Sci. Technol. 28 065012

(http://iopscience.iop.org/0268-1242/28/6/065012)

Semicond. Sci. Technol. **28** (2013) 065012 (5pp) doi:10.1088/0268-1242/28/6/065012

Optical fingerprints of Y2 ordering in III–V ternary semiconductor alloys

Dongguo Chen and N M Ravindra

Department of Physics, New Jersey Institute of Technology, Newark, NJ 07102, USA

E-mail: dc74@njit.edu

Received 16 January 2013, in final form 18 March 2013
Published 16 May 2013
Online at stacks.iop.org/SST/28/065012

Abstract

In this paper, we report the Y2 ordering induced changes in the crystal field splitting, spin–orbit splitting and band gap for $Al_xGa_{1-x}As$, $Ga_xIn_{1-x}As$, $Ga_xIn_{1-x}P$, $GaAs_xSb_{1-x}$ and InP_xSb_{1-x} using first-principles calculations. These values and the valence band splittings E_{12}, E_{13} for these materials are provided as a function of the ordering parameter η. The trends of these properties among materials are explained. The optical fingerprints of Y2 ordering are then compared with those of other available structures and the experimental data.

(Some figures may appear in colour only in the online journal)

1. Introduction

Spontaneous Y2 ordering of isovalent $A_xB_{1-x}C$ semiconductor alloys has been observed in vapor phase growth of some III–V systems [1–6]. However, the fundamental properties of this ordering have not been systematically studied. The ordered phase consists of alternate cation monolayer planes $A_{x+\eta/2}B_{1-x-\eta/2}$ and $A_{x-\eta/2}B_{1-x+\eta/2}$ stacked along the [1 1 0] direction, where $0 \leqslant \eta \leqslant 1$ is the long range order parameter. $\eta = 1$ corresponds to the fully ordered phase (figure 1(*a*)) and $\eta = 0$ corresponds to the fully disordered phase. The degree of ordering depends on the experimental conditions, such as, the growth temperature and pressure, growth rates and substrate orientation etc.

When a zincblende disordered alloy forms the long-range ordered Y2 phase, the unit cell is increased and the Brillouin zone is reduced. The point group symmetry is changed from T_d to C_{2v}. These lead to a series of experimental observable changes in materials properties, including a new photoluminescence and electroreflectance peak [1, 5], new x-ray diffraction spots at (1/2, 1/2, 0) [2, 4], new pressure deformation potential [7] and the shift of absorption edge [2]. In this work, we focus on the changes of optical properties near the absorption edge. These changes are due to the fact that, in the ordered phase, the Γ, X and Σ points in the zincblende binary constituents all fold into the Γ point at the Y2 Brillouin zone (figure 1(*b*)). These folding relations couple the states that have the same symmetry and this coupling splits the degenerate states in the random alloys.

In the absence of spin–orbit (SO) splitting, the valence band maximum (VBM) of the random alloy is a triply degenerate state with Γ_{15v} symmetry (figure 2(*a*)). In Y2 ordering, this state splits into a single state Γ_{1v} and a doubly degenerate state. The doubly degenerate state splits further into two single states Γ_{2v} and Γ_{3v} due to the yet lower symmetry (figure 2(*b*)). In the presence of SO splitting, the amount of splitting becomes more significant.

The valence band splittings can be expressed, in terms of the energies of the top three valence band states, $E_1(\Gamma_{1v})$, $E_2(\Gamma_{2v})$ and $E_3(\Gamma_{3v})$, as follows:

$$\begin{aligned} \Delta E_{12}(\eta) &= E_1(\Gamma_{1v}) - E_2(\Gamma_{2v}) \\ \Delta E_{13}(\eta) &= E_1(\Gamma_{1v}) - E_3(\Gamma_{3v}) \end{aligned} \tag{1}$$

Using the Hopfield quasicubic model [8], $\Delta E_{12}(\eta)$ and $\Delta E_{13}(\eta)$ for Y2 ordering are given by

$$\begin{aligned} \Delta E_{12}(\eta) &= \tfrac{1}{2}[\Delta_{SO}(\eta) + \Delta_{CF}(\eta)] \\ &\quad - \tfrac{1}{2}\left\{[\Delta_{SO}(\eta) + \Delta_{CF}(\eta)]^2 - \tfrac{8}{3}\Delta_{SO}(\eta)\Delta_{CF}(\eta)\right\}^{\frac{1}{2}} \\ \Delta E_{13}(\eta) &= \tfrac{1}{2}[\Delta_{SO}(\eta) + \Delta_{CF}(\eta)] \\ &\quad + \tfrac{1}{2}\left\{[\Delta_{SO}(\eta) + \Delta_{CF}(\eta)]^2 - \tfrac{8}{3}\Delta_{SO}(\eta)\Delta_{CF}(\eta)\right\}^{\frac{1}{2}} \end{aligned} \tag{2}$$

where $\Delta_{SO}(\eta)$ is the SO splitting and $\Delta_{CF}(\eta)$ is the ordering-induced crystal field (CF) splitting in the absence of SO splitting. $\Delta_{CF}(\eta)$ is defined to be negative if the doubly degenerate state is below the single state.

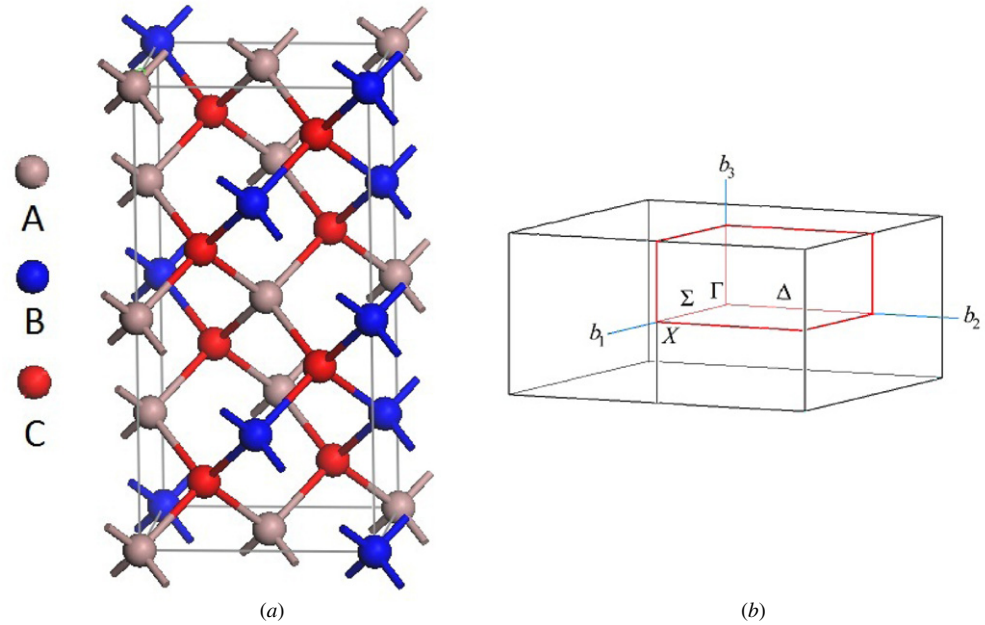

(*a*) (*b*)

Figure 1. (*a*) The crystal structure of ternary alloy $A_xB_{1-x}C$ in Y2 ordering; (*b*) the Brillouin zone of the Y2 ordered superlattice.

In the literature, Y2 ordering has been observed in five ternary compounds [1–6], i.e. $Al_xGa_{1-x}As$, $Ga_xIn_{1-x}As$, $Ga_xIn_{1-x}P$, $GaAs_xSb_{1-x}$ and InP_xSb_{1-x}. Here we report the optical fingerprints, including valence band splittings and band gap narrowing (the ordering induced band gap reduction relative to the random alloy), $\Delta E_g(\eta) = E_g(\eta) - E_g(0)$, of these five Y2 ordered compounds at partial and full degree of ordering. We will point out the physical factors that affect the optical fingerprints. Properties of materials in Y2 ordering will also be compared with properties of these materials in other observed orderings. Our calculated data can be useful in analyzing experimental observations and deriving the ordering parameters of partially ordered samples.

2. Method of calculation

The band-structure calculations are performed within the first-principles density functional formalism as implemented in the projector augmented wave method [9]. For the exchange-correlation potential, we use the generalized gradient approximation (GGA) of Perdew and Wang, known as PW91 [10]. The cutoff energies and size of k points are tested to ensure the total energies converge within 0.1 meV per atom. The Ga 3*d* and In 4*d* states are treated on the same footing as the other *s* and *p* valence states. The lattice constants of the alloys are determined from the linear interpolation of the experimental values [11] of the binary compounds.

3. Results and discussion

For a spontaneously formed partially ordered semiconductor alloy with $\eta \leqslant 1$, the physical properties $P(x, \eta)$, such as, the CF splitting $\Delta_{CF}(\eta)$, the SO splitting $\Delta_{SO}(\eta)$ and the band gap $E_g(\eta)$, at composition x can be described by [12]

$$P(x, \eta) = P(x, 0) + \eta^2[P(X_\sigma, 1) - P(X_\sigma, 0)] \qquad (3)$$

This equation shows that the property $P(x, \eta)$ of a semiconductor alloy $A_xB_{1-x}C$ can be calculated by (i) the corresponding properties $P(x, 0)$ of the random structure at the same composition x, (ii) the degree of ordering η, and (iii) the difference of the property, $P(X_\sigma, 1) - P(X_\sigma, 0)$, between the fully ordered structure and random structure at composition $X_\sigma = 0.5$.

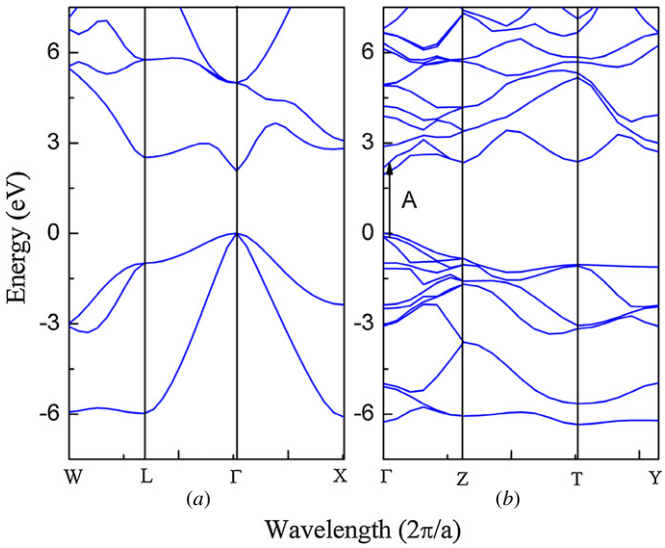

Figure 2. The band structures for the (*a*) random and (*b*) Y2 ordered $Ga_{0.5}In_{0.5}P$ alloy are plotted along the high symmetry lines in the Brillouin zone. The arrow A denotes the interband transition responsible for the anomalous peak at 2.2 eV in the electroreflectance spectra.

According to equations (1)–(3), if the valence band splitting, $\Delta E_{12}(\eta)$, $\Delta E_{13}(\eta)$, and band gap, $\Delta E_g(\eta)$, are known independently, for example, from electroreflectance or photoluminescence spectrum, the SO splitting $\Delta_{SO}(x, \eta)$ and CF splitting $\Delta_{CF}(x, \eta)$ can be derived according to equation (2). Then our theoretically calculated differences in the SO splitting, $[\Delta_{SO}(1) - \Delta_{SO}(0)]$, CF splitting,

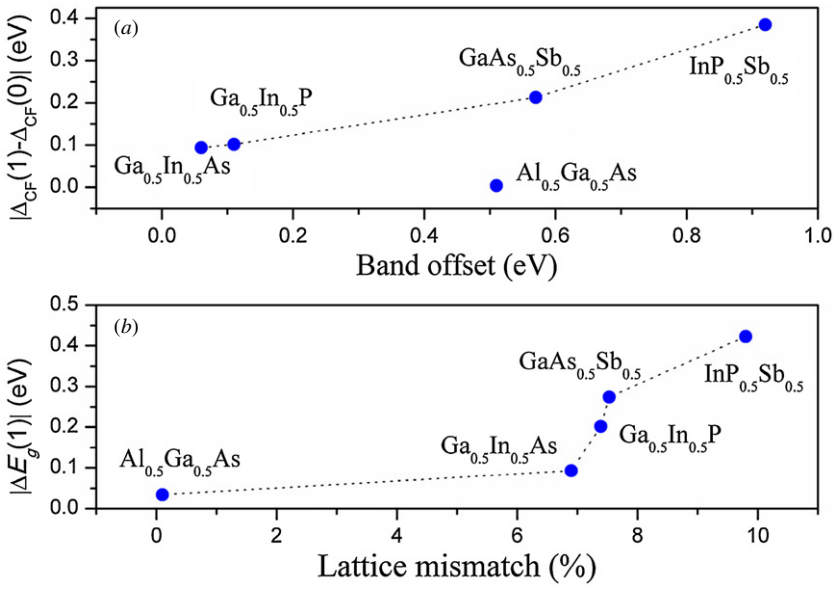

Figure 3. (*a*) Variation of the crystal field splitting $[\Delta_{CF}\ (1) - \Delta_{CF}\ (0)]$ with the band offset between alloys' binary constituents. (*b*) Variation of the band gap narrowing $\Delta E_g(1)$ with the alloys' lattice mismatch.

Table 1. GGA calculated optical fingerprints of five III–V alloys: valence band splitting, $\Delta E_{12}\ (1)$ and $\Delta E_{13}\ (1)$, changes in spin–orbit splitting $[\Delta_{so}(1) - \Delta_{so}(0)]$, crystal field splitting $[\Delta_{\rm CF}(1) - \Delta_{\rm CF}(0)]$ and band gap $\Delta E_g(1)$. Values are given in units of eV.

Alloys	$Al_{0.5}Ga_{0.5}As$	$Ga_{0.5}In_{0.5}As$	$Ga_{0.5}In_{0.5}P$	$GaAs_{0.5}Sb_{0.5}$	$InP_{0.5}Sb_{0.5}$
$\Delta E_{12}(1)$	0.009	0.129	0.091	0.188	0.357
$\Delta E_{13}(1)$	0.318	0.385	0.169	0.643	0.701
$\Delta_{so}(1) - \Delta_{so}(0)$	0.001	0.005	0.013	0.021	0.052
$\Delta_{CF}(1) - \Delta_{CF}(0)$	−0.004	−0.094	−0.102	−0.213	−0.385
$\Delta E_g(1)$	−0.034	−0.093	−0.202	−0.274	−0.423

$[\Delta_{CF}\ (1) - \Delta_{CF}\ (0)]$, and the band gap narrowing, $\Delta E_g\ (\eta)$, can be used to derive the ordering parameter η using equation (3). On the other hand, if η is available independently from experiment, such as x-ray diffraction, one can assess the valence band splitting, $\Delta E_{12}\ (\eta)$, $\Delta E_{13}\ (\eta)$, and band gap narrowing $\Delta E_g\ (\eta)$.

The results of the GGA calculations are shown in table 1. We find the following.

(i) Ordering induces a decrease in band gap and CF splitting, but an increase in SO splitting in all the five alloy systems.

(ii) $[\Delta_{SO}\ (1) - \Delta_{SO}\ (0)]$ is always positive. This is due to the fact that the VBM wave function of the ordered compounds, relative to the random alloy, is more localized on the cation atom with larger atomic number [13]. For common-anion systems, the two binary constituents have similar Δ_{SO}. Therefore, the ordering induced difference $[\Delta_{SO}\ (1) - \Delta_{SO}\ (0)]$ is rather small. However, the common-cation systems (e.g. $GaAs_{0.5}Sb_{0.5}$ and $InP_{0.5}Sb_{0.5}$) have relatively larger $[\Delta_{SO}\ (1) - \Delta_{SO}\ (0)]$, because they have larger anion atom Sb. The SO splitting increases monotonically when anion atomic number increases [13].

(iii) As shown in figure 3(*a*), the CF splitting $[\Delta_{CF}\ (1) - \Delta_{CF}\ (0)]$ increases in the following sequence: $Ga_{0.5}In_{0.5}As \rightarrow Ga_{0.5}In_{0.5}P \rightarrow GaAs_{0.5}Sb_{0.5} \rightarrow InP_{0.5}Sb_{0.5}$. According to the perturbation theory, Δ_{CF} is proportional to the valence band offset and inversely proportional to the difference between the symmetric energy levels of binary constituents [14]. The band offset of a semiconductor alloy AB_xC_{1-x} refers to the relative alignment of the valence band maxima of the corresponding constituents AB and AC. This can explain the trend in CF splitting. For example, the band offset [15] between GaAs and GaSb for $GaAs_{0.5}Sb_{0.5}$ (0.57 eV) is much larger than that between GaAs and InAs for $Ga_{0.5}In_{0.5}As$ (0.06 eV). Therefore, the perturbation and CF splitting in the valence bands are larger in $GaAs_{0.5}Sb_{0.5}$ than in $Ga_{0.5}In_{0.5}As$. Note that the band offset between AlAs and GaAs for $Al_{0.5}Ga_{0.5}As$ is rather large (0.51 eV). It still, however, has the smallest $[\Delta_{CF}\ (1) - \Delta_{CF}\ (0)]$ at Γ point of its Brillouin zone, as shown in table 1 and figure 3(*a*). This is because $Al_{0.5}Ga_{0.5}As$ compound has an indirect band gap in this ordering.

(iv) The band gap narrowing $\Delta E_g\ (\eta)$ increases with the increasing of the alloy lattice mismatch between the binary constituents, as shown in figure 3(*b*). For example, the lattice mismatch between the binary constituents for $Al_{0.5}Ga_{0.5}As$ and $Ga_{0.5}In_{0.5}As$ are 0.14% and 6.92%, respectively, smaller than that of 9.88% between InP and InSb for $InP_{0.5}Sb_{0.5}$ compound. During the formation of the lattice mismatch alloys, the structure relaxation tends to shift the charge from the long bond to the short bond and thus reduce the repulsion between the symmetric energy

Table 2. Calculated properties of fully Y2 ordered five compounds. Results of CA, CH and CP orderings of GaInP and GaAsSb are also listed for comparison. The units are Å for lattice constant a and eV for crystal field splitting Δ_{CF}, spin–orbit splitting Δ_{SO} and its bowing parameter $b\,(\Delta_{SO})$.

Alloys	Structure	a	Δ_{CF}	Δ_{SO}	$b\,(\Delta_{SO})$
$Ga_{0.5}In_{0.5}P$	Y2	5.6599	−0.102	0.104	−0.053
$Ga_{0.5}In_{0.5}P$	CA	5.6599	0.199	0.097	−0.023
$Ga_{0.5}In_{0.5}P$	CH	5.6599	−0.015	0.093	−0.008
$Ga_{0.5}In_{0.5}P$	CP	5.6599	0.232	0.103	−0.047
$GaAs_{0.5}Sb_{0.5}$	Y2	5.8746	−0.213	0.539	−0.084
$GaAs_{0.5}Sb_{0.5}$ [14]	CA	5.8927	0.085	0.549	−0.10
$GaAs_{0.5}Sb_{0.5}$ [14]	CH	5.8922	−0.013	0.521	−0.01
$GaAs_{0.5}Sb_{0.5}$ [14]	CP	5.8974	0.230	0.605	−0.33
$Al_{0.5}Ga_{0.5}As$	Y2	5.5659	−0.004	0.316	−0.005
$Ga_{0.5}In_{0.5}As$	Y2	5.8558	−0.094	0.343	−0.019
$InP_{0.5}Sb_{0.5}$	Y2	6.1740	−0.385	0.467	−0.208

levels. This repulsion lowers the Γ_{1c} state and raises the Γ_{VBM} state, resulting in a band gap narrowing. In alloys with larger lattice mismatch between the constituents, more charge is transferred and therefore the band gap narrowing is larger.

Numerous studies [16–19] on the ordering of the alloy $Ga_{0.5}In_{0.5}P$ have reported the CuPt (CP, $R3m$) structure and, however, ignored the Y2 ordering. This is due to the similarity between CuPt and Y2 orderings. They are built from the same (0 0 1) plane and differ only in the stacking of the subsequent planes. In fact, some reports [20, 21] have mistakenly attributed the extra features in the spectra originated from Y2 ordering into CuPt ordering. Moreover, the small difference between the formation enthalpies of CuAu-I (CA, $P\bar{4}m2$) and Y2 ordering in some alloys may also cause the co-existence of CA and Y2 orderings [4]. In view of these facts, we compare the optical fingerprints of Y2 ordering with those of CA, CP and chalcopyrite (CH, $I\bar{4}2d$) structures. The structure information of CA, CP and CH orderings can be found in [14]. Results are listed in table 2. We find the following.

(i) Relative to other orderings, Y2 ordering has large and negative CF splitting Δ_{CF}. As it has been highlighted before, the ordering separates the triply degenerate states in random alloy into a single state and a doubly degenerate state. In CA and CP orderings, the doubly degenerate state is above the single state, resulting in a positive CF splitting. However, in CH and Y2 ordering, the doubly degenerate state is below the single state, resulting in a negative CF splitting. In Y2 ordering, the doubly degenerate state splits further into two single states. Due to the smaller difference in the symmetric energy levels of the binary constituents in Y2 ordering than in CH ordering, the CF splitting is larger in Y2 ordering.

(ii) The bowing parameter of SO splitting is negative in Y2 ordering. The compositional variation of the SO splitting for alloy $A_xB_{1-x}C$ can be fitted to the form:

$$\Delta_{SO}(x) = \overline{\Delta}_{SO}(x) - x(1-x)b(\Delta_{SO}) \qquad (4)$$

where, $\overline{\Delta}_{SO}(x)$ is the concentration-weighted average SO splitting. SO splitting reflects the way that bonding in solids redistributes the charge around the atomic cores of the constituents [22]. The sign of the SO splitting bowing parameter reflects the alloy environment acting to enhance or diminish the magnitude of SO splitting beyond the linear average of the constituents. Our calculation shows that formation of Y2 ordering enhances the magnitude of Δ_{SO} and yields a negative SO splitting bowing parameter $b(\Delta_{SO})$. This is in contradiction with the results of most early experimental measurements [23, 24], but consistent with more recent data [25–27]. The negative sign of $b(\Delta_{SO})$ is also proposed, by Wei *et al* [28], for the other CA, CH and CP orderings of $GaAs_{0.5}Sb_{0.5}$ compounds and this upward concave bowing is attributed to the intraband p–p coupling.

4. Comparison with experiment

Using the electroreflectance spectroscopy method, Kurtz [1] found an anomalous peak at about 2.2 eV in spontaneously ordered $Ga_{0.5}In_{0.5}P$ alloy. This peak is attributed to the X point folding to Γ point in the first Brillouin zone due to the Y2 ordering. According to our calculated band structures, this peak corresponds to the transition (denoted as A in figure 2(b)) from the second and third VBM states to the second conduction band minimum state. Our calculated value for transition A is 2.27 eV, in good agreement with the experimental result of 2.2 eV. The band diagram, produced by Kurtz [1], using virtual crystal approximation method, suggests that Y2 ordering in $Ga_{0.5}In_{0.5}P$ will result in a band gap narrowing of 0.17 eV. This value is close to our GGA calculated data of 0.202 eV. Using transmission electron microscopy and photoluminescence methods, Gomyo *et al* [2] reported a band gap narrowing of 0.05 eV for $Ga_{0.5}In_{0.5}P$ due to the partially Y2 ordering. According to our calculations, the sample should have ordering η around 0.5.

Our calculated values of valence band splittings, $\Delta E_{12}\,(1) = 0.091$ eV and $\Delta E_{13}\,(1) = 0.169$ eV, for fully Y2 ordered $Ga_{0.5}In_{0.5}P$ are consistent with the results, 0.10 and 0.15 eV, reported by Lee *et al* [29]. The calculated values of CF splitting and SO splitting are also in good accord with the available experimental results. For example, the reported [23, 30] SO splitting for $Ga_{0.5}In_{0.5}As$ are 0.345 and 0.33 eV while our calculations obtained 0.343 eV. The calculated bowing parameter of SO splitting for $Ga_{0.5}In_{0.5}P$ is –0.053 eV. This value is very close to the measured result of –0.05 eV using the electroreflectance and wavelength modulation methods [25].

Recently, Wu *et al* [3] reported the observation of Y2 ordering in $InP_{0.52}Sb_{0.48}$. Using reciprocal space mapping and extended x-ray absorption fine structure method, they found the structure parameter $c/a = 1.009$. This is considerably larger than our predicted value of 0.997 (not listed) for $InP_{0.5}Sb_{0.5}$. However, they find that the strong distorted In–P and In–Sb bonds prevent the crystal lattice from full relaxation. This may explain the difference between our calculated result and their measured value.

5. Summary

We have calculated the Y2 ordering induced changes in the optical fingerprints, including crystal field splitting, spin–orbit splitting, band gap and valence band splittings, for $Al_xGa_{1-x}As$, $Ga_xIn_{1-x}As$, $Ga_xIn_{1-x}P$, $GaAs_xSb_{1-x}$ and InP_xSb_{1-x} using first-principles calculations. These values for the five materials are provided as a function of the degree of long range order η. For the partially ordered samples, we explain the trends of the changes in the crystal field splitting and band gap narrowing. The change of spin–orbit splitting is found to be positive and small. For the fully ordered samples, we compare Y2 with other orderings and find that Y2 has a large and negative crystal field splitting and negative spin–orbit bowing parameter. Our calculated data can be useful in analyzing experimental results and deriving the ordering parameters of partially ordered samples.

Acknowledgement

The authors gratefully thank Professor Keun Hynk Ahn from Department of Physics at New Jersey Institute of Technology for useful discussions.

References

[1] Kurtz S 1993 *J. Appl. Phys.* **74** 4130
[2] Gomyo A, Suzuki T, Kobayashi K, Kawata S, Hino I and Yuasa T 1987 *Appl. Phys. Lett.* **50** 673
[3] Wu C, Feng Z, Chang W, Yang C and Lin H 2012 *Appl. Phys. Lett.* **101** 091902
[4] Kuan T S, Kuech T F, Wang W I and Wilkie E L 1985 *Phys. Rev. Lett.* **54** 201
[5] Ruvimov S *et al* 1995 *Phys. Rev.* B **51** 14766
[6] Zhong Z, Li J H, Kulik J, Chow P C, Norman A G, Mascarenhas A, Bai J, Golding T D and Moss S C 2001 *Phys. Rev.* B **63** 033314
[7] Franceschetti A and Zunger A 1994 *Appl. Phys. Lett.* **65** 2990
[8] Hopfield J J 1960 *J. Phys. Chem. Solids* **15** 97
[9] Blochl P E 1994 *Phys. Rev.* B **50** 17953
[10] Perdew J P, Chevary J A, Vosko S H, Jackson K A, Pederson M R, Singh D J and Fiolhais C 1992 *Phys. Rev.* B **46** 6671
[11] Adachi S 2004 *Handbook on Physical Properties of Semiconductors* vol 1 (Boston: Kluwer Academic)
[12] Wei S, Laks D B and Zunger A 1993 *Appl. Phys. Lett.* **62** 1937
Wei S, Laks D B and Zunger A 1993 *Appl. Phys. Lett.* **63** 1292 (erratum)
[13] Carrier P and Wei S 2004 *Phys. Rev.* B **70** 035212
[14] Wei S and Zunger A 1989 *Phys. Rev.* B **39** 3279
[15] Wei S and Zunger A 1998 *Appl. Phys. Lett.* **72** 2011
[16] Suzuki T, Gomyo A, Iijima S, Kobayashi K, Kawata S, Hino I and Yuasa T 1988 *Japan. J. Appl. Phys.* **27** 2098
[17] Morita E, Ikeda M, Kumagai O and Kanedo K 1988 *Appl. Phys. Lett.* **53** 2164
[18] Baxter C S, Broom R F and Stobbs W M 1990 *Surf. Sci.* **228** 102
[19] Baxter C S, Stobbs W M and Wilkie J H 1991 *J. Cryst. Growth* **112** 373
[20] Inoue Y, Nishino T, Hamakawa Y, Kondow M and Minagawa S 1988 *Optoelectronics* **3** 61
[21] Inoue Y, Hamakawa Y, Kondow M and Minagawa S 1988 *Appl. Phys. Lett.* **53** 583
[22] Phillips J C 1973 *Bonds and Bands in Semiconductors* (New York: Academic)
[23] Berolo O and Woolley J C 1972 *Proc. 11th Int. Conf. on the Physics of Semiconductors* ed M Miasek (Polish Scientific: Warsaw)
[24] Van Vechten J A, Berolo O and Woolley J C 1972 *Phys. Rev. Lett.* **29** 1400
[25] Lange H, Donecker J and Friedrich H 1976 *Phys. Status Solidi* b **73** 633
[26] Thompson A G, Cardona M, Shaklee K L and Woolley J C 1966 *Phys. Rev.* **146** 601
[27] Ebina A, Sato Y and Takahashi T 1974 *Phys. Rev. Lett.* **32** 1366
[28] Wei S and Zunger A 1989 *Phys. Rev.* B **39** 6279
[29] Lee K, Lee S and Chang K J 1995 *Phys. Rev.* B **52** 15862
[30] Nee T W and Green A K 1990 *J. Appl. Phys.* **68** 5314